

Received April 16, 2019, accepted May 3, 2019, date of publication May 8, 2019, date of current version June 11, 2019.

Digital Object Identifier 10.1109/ACCESS.2019.2915528

Economic Dispatch of Grid-Connected Microgrid for Smart Building Considering the Impact of Air Temperature

MOHAMAD ABU HOURAN¹, WENJIE CHEN¹, MINGHUI ZHU², AND LIYU DAI¹

¹Department of Electrical Engineering, Xi'an Jiaotong University, Xi'an 710049, China

²State Grid Shaanxi Electric Power Research Institute, Xi'an 710100, China

Corresponding author: Wenjie Chen (cwj@xjtu.edu.cn)

ABSTRACT The economic dispatch (ED) operation is based on determining the optimal output of all the distributed energy resources (DERs) of a microgrid to meet the load demand at the lowest cost. In this paper, a smart commercial building model is supplied by several distributed generations (DGs), for example, PV power plants, diesel generators, and energy storage system (ESS). In addition, the microgrid is connected to the main grid (grid-connected mode), which allows the system to trade power with the main grid. The aim of this paper is managing DERs that operate over a time horizon and satisfy several key constraints at the lowest possible cost. Therefore, an improved energy management (EM) operation is proposed to achieve better energy efficiency in the building. In the proposed EM operation, the ED problem is investigated according to several aspects, such as the impact of air temperature, thermal resistance (R) of the building envelope, and time horizon (day-ahead ED and five-minute-ahead ED). Finally, the results of the general algebraic modeling system (GAMS) are used to validate the accuracy and feasibility of the proposed EM operation.

INDEX TERMS Economic dispatch, energy management, impact of air temperature, microgrid, smart building.

I. INTRODUCTION

The load demand is increasing rapidly, especially in the building sector, which is considered one of the biggest consumers of energy. The research approaches mostly focus on the energy conservation, energy efficiency, and using the renewable clean energy [1]. Regarding the energy-saving solutions in the building sector, it can be classified into two categories. The first is passive solutions, which include permanent procedures, for example, the building insulation or using insulated glazing. The second is using automated systems, such as controlled lighting systems, shading systems, and thermal loads that follow a desired internal temperature [2]. Smart buildings have some DERs, such as ESS system or renewable energy resources. In addition, it is connected to the main grid to trade power. Moreover, diesel generators and CHP are used as reserve generation [3]. Smart building provides an energy-efficient living and environment-friendly place [4]. ED problem is based on finding the optimal combination of DERs

to reduce the cost. Some constraints, such as supply-demand and operation constraints are considered [5].

Many studies have been conducted in this field, for example, a low-energy consumption building is given in [6]. It is supplied by DGs. However, profiles of thermal and electrical loads are already given. In [7], Mohammad *et al.* studied a building that is provided by smart meters and controllable electrical loads to engage the smart control for the microgrid. In this study, the required thermal power is given for the heating load. A microgrid operates in the islanded state is discussed in [8]. However, ESS is not investigated and the thermal load is considered constant. Moreover, an isolated microgrid that supplies three remote areas is given [9]. Same case is introduced in Budapest as well [10]. However, these studies did not include thermal load assessments. In [11] and [12], the authors presented a renewable-based microgrid with a storage system. The cogeneration or the micro-turbine problems are not considered. In [13] and [14], the cost function of the micro-turbine is given as a linear function. However, in this paper, it is given as a quadratic equation.

The associate editor coordinating the review of this manuscript and approving it for publication was Emanuele Lattanzi.

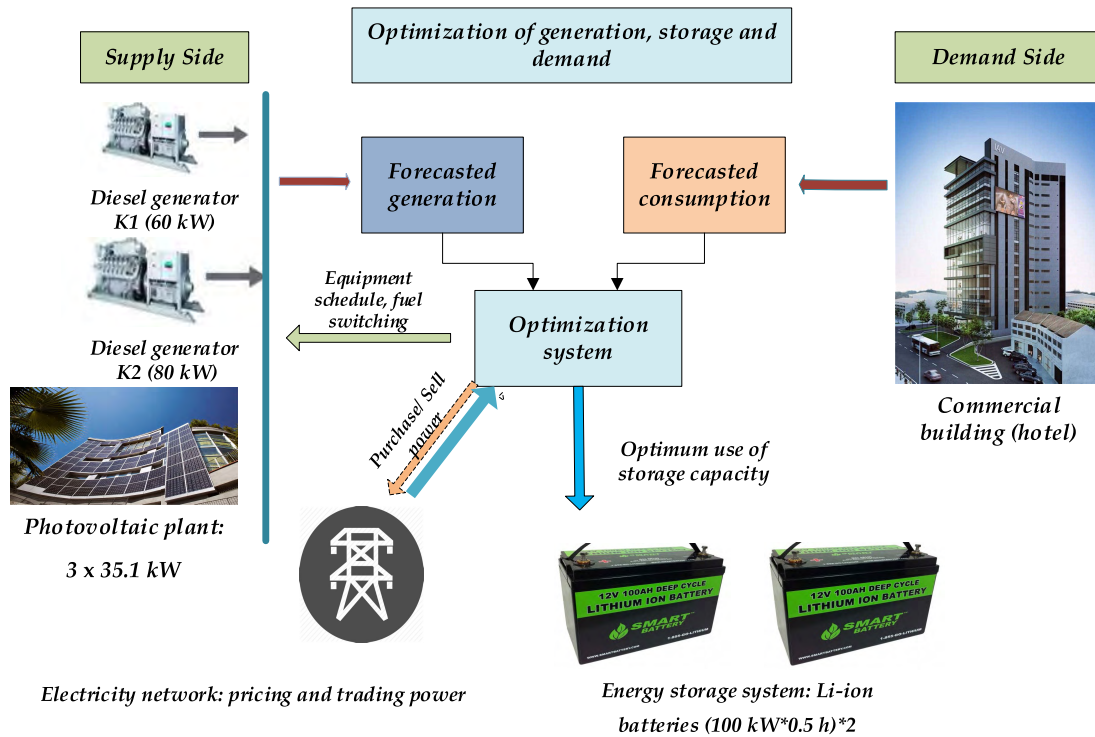


FIGURE 1. Smart building network (supply-demand).

The accuracy and feasibility of ED are validated by software, such as HOMER software in grid-connected state [15]. Many ED aspects are given, for example, power trade, scheduling, and demand side management (DSM) [16], [17]. Finally, many studies related to dispatch interval have been investigated, for instance, day-ahead EM operation strategy [6], [18], [19], [20], and two-day ahead ED [21]. Moreover, fifteen-minute ahead [22], and ultra-short term EM [23], [24] are reported.

On considering the abovementioned problems, this paper aims to manage DERs and minimize the total cost of energy in the studied building. Therefore, an improved EM operation is proposed. In the proposed model, the electrical and thermal load profiles are considered. In addition, day ahead and five-minute ahead ED operations are discussed in detail with respect to some constraints, such as power generation, power price, power balance, and ESS control constraints. Furthermore, weather condition (air temperature) impact on the EM operation is investigated. Therefore, the air temperature impact on thermal loads is carried out in detail. Finally, effects of the thermal resistance (R) of the building envelope is discussed.

The paper is organized as follows. Section II presents the EM model of the key elements in the smart building. The mathematical model formulation including several constraints is given in section III. The improved model considering the air temperature impact is discussed in section IV. The simulation results and case studies are investigated in section V.

II. THE ENERGY MANAGEMENT MODEL OF DISTRIBUTED GENERATIONS OF THE MICROGRID

Fig. 1 represents an electrical network with DGs on the supply side. The network includes two diesel generators and three PV power plants. On the other hand, the demand side represents the building systems, such as lighting and HVAC. Moreover, the building is connected to the utility grid, which allows the customer to purchase or sell electricity (bidirectional energy flow). In addition, there is an ESS, which gives more flexibility to the microgrid.

A. DIESEL GENERATORS

Cost function of diesel generator is given as a nonlinear quadratic equation in (1) [25], [26]. Where $P_{di}(t)$ is the output power at dispatch period t (kW). a, b, c are the cost function coefficients, and their units are as follows: USD/ kW²h, USD/ kWh and USD/h, respectively.

$$F_{DGi}(t) = a P_{di}^2(t) + b P_{di}(t) + c \quad (1)$$

B. PV SYSTEM DATA

The combination of renewable energy sources results in more uncertainty to the microgrid operation because the output power relies on the weather conditions, such as the wind speed and sun radiation. However, the renewable sources play an essential role in ED operation. The proposed microgrid system has three PV plants (3 × 35.1 kW). The solar radiation data is converted into output power by (2) [26]. The calculated

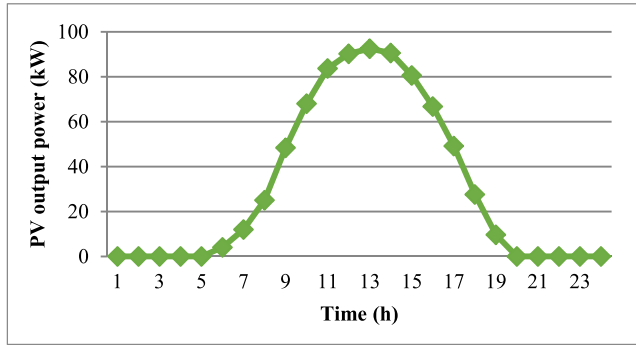


FIGURE 2. Calculated PV output power.

TABLE 1. Electricity price.

Period	Time (hour)	Purchase price (USD/ kW)	Sell price (USD/ kW)
On-peak	10.00-17.00	0.08	0.06
Off-peak	The rest	0.04	0.06

output power is illustrated in Fig. 2.

$$P_{PV} = P_{STC} \frac{G_{ac}}{G_{STC}} (1 + K(T_c - T_i)) \quad (2)$$

P_{PV} is PV output power (kW), and P_{STC} is the maximum power of PV at STC (kW). G_{ac} is the incident solar irradiation (W/m^2), and G_{STC} solar irradiance at STC, which is $1000 W/m^2$ and $25^\circ C$. In addition, K is temperature coefficient (-0.0047), and T_i, T_c are the reference and cell temperatures, respectively ($^\circ C$).

C. PURCHASED/SOLD POWER FROM/TO UTILITY GRID

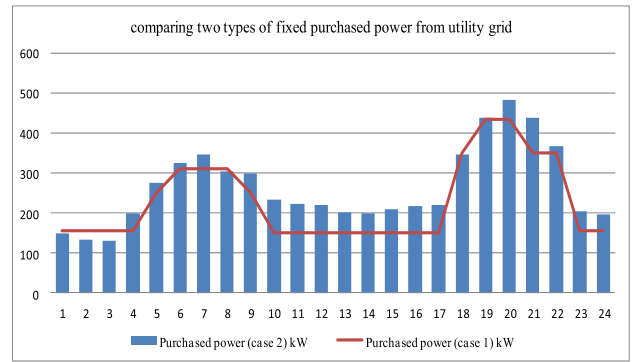
In this paper, two cases of utility grid power are investigated. They are fixed and variable power curves. The first is fixed purchased power curve, which concludes two scenarios: day-ahead ED and five-minute ahead ED as displayed in Fig. 3 (a), Fig. 3 (b), respectively. The second is the variable power curve, which is affected by power price. The electricity prices during the on-peak time will be high. However, during the off-peak time, the price will be low. As given in table 1, on-peak time is 10.00 am –17.00 pm.

D. ENERGY STORAGE SYSTEM (ESS)

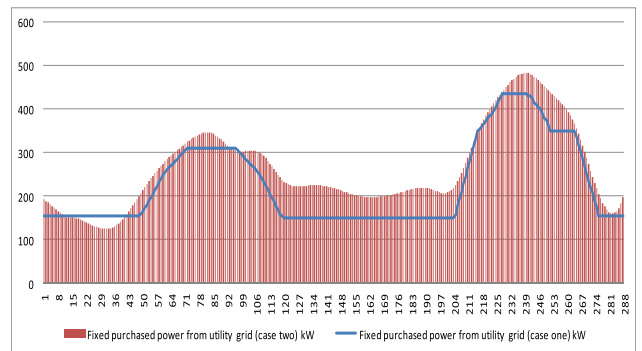
To use ESS optimally, it is essential to find out the optimal discharging and charging schemes for the devices, which take into consideration the dynamic environment. Rechargeable Li-ion batteries are used. Battery data is presented in Table 2 [27].

E. DEMAND SIDE: END USE LOAD

Electrical and thermal load profiles are discussed. The electrical demand is given in table 3. The thermal demand, which means the air conditioning load for space cooling and space heating (HVAC) will be calculated.



(a)



(b)

FIGURE 3. Purchased Power. (a) Day-ahead ED. (b) Five-minute ahead ED.

TABLE 2. Battery data.

ESS parameters	Explanation	Electrical
Maximum charging rate	Maximum portion of added rated capacity to the storage during an hour	0.25
Maximum discharging rate	Maximum portion of withdrawn rated capacity from storage during an hour	0.25
Minimum state of charge	rated capacity portion	0.3

III. ED PROBLEM FORMULATION

ED problem is a complex operation due to its large dimension, including many constraints. Moreover, it has a non-linear objective function. Therefore, general algebraic modeling system (GAMS) is used. GAMS is useful when dealing with large complex problems, such as modeling nonlinear problems, linear problems, or mixed integer optimization problems (MIO). The basic mathematical model structure, which is coded in GAMS, has the following components: sets, data, variables, equations, model, and output.

A. OBJECTIVE FUNCTION

The total cost includes the cost of power generation of diesel generators, maintenance and operation cost (M + O), the cost of purchased power, and the obtained gain by selling energy to the grid. Therefore, the ED objective function of

TABLE 3. Electrical demand.

Time (h)	1:00	2:00	3:00	4:00	5:00	6:00	7:00	8:00	9:00	10:00	11:00	12:00
Demand (kW)	215	205	200	280	350	425	470	435	425	350	375	360
Time (h)	13:00	14:00	15:00	16:00	17:00	18:00	19:00	20:00	21:00	22:00	23:00	24:00
Demand(kW)	330	340	343	360	350	495	560	575	503	444	270	240

grid-connected mode can be formulated as given in (3) [6], [28].

$$\begin{aligned} \min C_T(p) &= \sum_{t=1}^T \left(\sum_{i=1}^n [F_i(P(t)) + COM_i(P(t))] + \right. \\ & \left. C_{buy}(t)P_{buy}(t) - C_{sell}(t)P_{sell}(t) \right) \\ &= \sum_{t=1}^T \sum_{i=1}^n (F_i(P(t)) + K_{COMi}P(t)) \\ & \quad + \sum_{t=1}^T (C_{buy}(t)P_{buy}(t) - C_{sell}(t)P_{sell}(t)) \quad (3) \end{aligned}$$

where $C_T(p)$ is the total cost function of the connected microgrid (USD), i is generator index, n is number of DGs, t is time interval, and T is the total interval time. In addition, $P(t)$ is output power of DG at time t (kW), and $F_i(P(t))$ is fuel cost of each generator at t (USD). COM_i is maintenance and operation costs of unit i (USD). K_{COMi} is proportional constant of the generation unit i . $C_{buy}(t)$, $C_{sell}(t)$ are the purchased and sold electricity prices at t (USD), respectively. $P_{sell}(t)$, $P_{buy}(t)$ are the sold and purchased powers at t (kW).

The cost function is formed by summing two parts. The first is $\sum_{t=1}^T \sum_{i=1}^n (F_i(P(t)) + K_{COMi}P(t))$, which represents the sum of the cost function of every generator, in addition to the maintenance and operation cost. The second is $\sum_{t=1}^T (C_{buy}(t)P_{buy}(t) - C_{sell}(t)P_{sell}(t))$, which represents the exchange power with utility grid, and depends on the price of electricity.

B. CONSTRAINTS

1) POWER BALANCE

Generated power on the supply side should be equal to the power on the demand side. Therefore, it is given as follows.

$$\begin{aligned} [P_{buy}(t) - P_{sell}(t) + P_{solar}(t) + P_{diesel}(t) + P_{batt}(t)] \\ = P_L(t) = P_{light}(t) \quad \forall t \in \{0, 1, \dots, T\} \quad (4) \end{aligned}$$

$$P_g(t) = P_{buy}(t) - P_{sell}(t) \quad \forall t \in \{0, 1, \dots, T\} \quad (5)$$

where $P_g(t)$ is purchased or sold power from/to utility grid at t (kW), P_{solar} is output power of PV plants at t (kW), $P_{diesel}(t)$ is power from diesel generators at t (kW), and $P_{batt}(t)$ is batteries output at t (kW). In addition, $P_L(t)$ is the electrical load at t (kW), and $P_{light}(t)$ is lighting load at time t (kW).

2) POWER GENERATION CONSTRAINT

To ensure the stability of system operation, each power generation should have maximum and minimum limits.

$$P_i^{\min} \leq P_i \leq P_i^{\max}, \quad \forall i = 1, 2, 3, \dots, N \quad (6)$$

where P_i^{\min} and P_i^{\max} are the minimum output power and maximum output power of unit i (kW).

3) ELECTRICITY COST FROM UTILITY GRID

$$C_T^p(t) = \begin{cases} C_{buy}(t)P_g(t) & \text{if } \cdot P_g \geq 0 \\ C_{sell}(t)P_g(t) & \text{if } \cdot P_g < 0 \end{cases} \quad \forall t \in \{0, 1, \dots, T\} \quad (7)$$

where $C_T^p(t)$ is the total cost of electricity at t (USD). The positive value of the grid power means that the power is purchased. However, the negative value means that the power is sold to the grid.

4) CONTROL CONSTRAINTS OF ESS

It includes the capacities of input power and output power, state of charge (SOC), and dynamics of SOC.

• Input and output power capacity

$$P_{batt}(t) \in \left\{ 0, \left[-P_{dis}^{\max}, -P_{dis}^{\min} \right], \left[P_{ch}^{\min}, P_{ch}^{\max} \right] \right\} \quad \forall t \in \{0, 1, \dots, T\} \quad (8)$$

if $\cdot P_{batt}(t) > 0 \rightarrow$ The battery charges.

if $\cdot P_{batt}(t) < 0 \rightarrow$ The battery discharges.

if $\cdot P_{batt}(t) = 0 \rightarrow$ The battery is idle.

where $P_{ch}^{\max}(t)$ and $P_{ch}^{\min}(t)$ are the the maximum battery charge and minimum battery charge (kW), respectively. $P_{dis}^{\max}(t)$ and $P_{dis}^{\min}(t)$ are the the maximum battery discharge and minimum battery discharge (kW), respectively.

• SOC constraint

$$x_{batt-\min}(t) = \frac{e_{critical}}{e_{batt-cap}} \leq x_{batt}(t) \leq 1 \quad \forall t \in \{0, 1, \dots, T\} \quad (9)$$

where $x_{batt-\min}$ is the lower limit of SOC, $x_{batt}(t)$ is battery SOC, $e_{critical}$ is the electrical consumed energy of critical loads (kW), and $e_{batt-cap}$ is battery capacity (kW).

• SOC dynam

$$x_{batt}(t+1) = x_{batt}(t) + \frac{P_{batt}(t) \cdot \tau}{e_{batt-cap}} \quad \forall t \in \{0, 1, \dots, T\} \quad (10)$$

where τ is the time period. The initial SOC: $x_{batt}(0)$ is assumed as (0.6).

The objective function and its constraints give a non-linear problem. Therefore, in order to linearize the problem, some binary variables are given in order to solve it faster. A general mixed integer programming (MIP) is used to solve the problem with appropriate discrete variables as follows.

$r_{buy}(t)$ is (1) if the system purchases power from grid at t , or else (0).

$r_{sell}(t)$ is (1) if the microgrid sells power to the grid at t , or else (0).

$r_{ch}(t)$ is (1) when the battery charges at t , or else (0).

$r_{dis}(t)$ is (1) when the battery discharges at t , or else (0).

As a result, the operating state of the main grid is written as follows.

$$r_{buy}(t) + r_{sell}(t) \leq 1 \quad \forall t \in \{0, 1, \dots, T\} \quad (11)$$

In addition, the electrical energy cost is given in (12). Finally, the input and output power capacities of the batteries are obtained by (13).

$$C_T^P(t) = (C_{buy}(t).P_{buy}(t) + C_{sell}(t).P_{sell}(t)).\tau$$

$$0 \leq P_{buy}(t) \leq r_{buy}(t).(+\infty)$$

$$0 \leq P_{sell}(t) \leq r_{sell}(t).(+\infty) \quad \forall t \in \{0, 1, \dots, T\} \quad (12)$$

$$\begin{cases} r_{ch}(t) + r_{dis}(t) \leq 1 \\ r_{ch}(t).P_{ch}^{min} - r_{dis}(t).P_{dis}^{max} \leq P_{batt}(t) \\ P_{batt}(t) \leq r_{ch}(t).P_{ch}^{max} - r_{dis}(t).P_{dis}^{min} \end{cases} \quad (13)$$

IV. IMPROVED MODEL WITH AIR TEMPERATURE IMPACT

Since there is a heat exchange between the external and internal environments of the building through the walls and windows. Outdoor temperature will affect the amount of the required energy to maintain the indoor temperature at a desired level. In this case, the cost function does not change. However, the amount of consumed energy will change according to the weather condition, which is represented by the outdoor air temperature. Consequently, the total cost will decrease or increase in accordance.

A. SUPPLY- DEMAND BALANCE

The balance between generation and demand will change as follows:

$$\begin{cases} [P_{buy}(t) - P_{sell}(t) + P_{solar}(t) +] \\ [P_{diesel}(t) + P_{batt}(t) \\ P_{light}(t) + P_{HVAC}(t) \end{cases} = \quad (14)$$

where $P_{HVAC}(t)$ is HVAC load demand at t (kW).

B. REQUIRED POWER FOR HEATING SPACE AND COOLING SPACE

The indoor temperature is given by [7].

$$T_{in}(t+1) = \left\{ \begin{array}{l} [T_{in}(t) \exp(-\Delta/\tau th) + \\ (R.P_{air}(t) + T_{out}(t)). \\ (1 - \exp(-\Delta/\tau th)) \end{array} \right\} \quad (15)$$

TABLE 4. Parameters of diesel generators.

P_{min} kW	P_{max} kW	M+O cost USD/ kW	Startup cost(\$)	Coefficients		
				a \$/ kW ² h	b \$/ kWh	c \$/h
12	60	0.001258	0.25	0.00033	0.0364	0.6339
16	80	0.001260	0.25	0.00027	0.0378	0.649

TABLE 5. Thermal parameters.

Parameter	Value	Unit
Desired Temperature	24	(°C)
R	10	(°C/kW)
C_{air}	0.525	(kWh/°C)
efficiency	50 %	-----
$T_{in\ min}$	23	(°C)
$T_{in\ max}$	26	(°C)

$$\tau th = R.C_{air} \quad (16)$$

where Δ is time interval (it is one hour in this case), τth is thermal constant, and R is the thermal resistance (°C/kW). Moreover, C_{air} is the cooling or heating capacity of the indoor air (kWh/°C), and T_d is the desired indoor temperature (°C). $T_{in}(t)$ and $T_{out}(t)$ are the indoor temperature and outdoor temperature at t (°C), respectively. $P_{air}(t)$ is thermal power, which is required to maintain the indoor temperature at the desired value (kW). The required power for heating and cooling systems are derived.

$$P_{heating}(t) = \left\{ \begin{array}{l} T_{in}(t+1) \\ - [T_{in}(t) \exp(-\Delta/\tau th)] - \\ [T_{out}(t) \cdot (1 - \exp(-\Delta/\tau th))] \end{array} \right\} / R.(1 - \exp(-\Delta/\tau th))$$

$$\forall t \in \{0, 1, \dots, T\} \quad (17)$$

$$P_{cooling}(t) = \left\{ \begin{array}{l} T_{in}(t+1) \\ -T_{in}(t) + T_{out}(t) - (T_{in}(t) \times \\ (1 - \exp(-\Delta/\tau th)) \end{array} \right\} / R.(1 - \exp(-\Delta/\tau th))$$

$$\forall t \in \{0, 1, \dots, T\} \quad (18)$$

where $P_{heating}(t)$ and $P_{cooling}(t)$ are the heating and cooling powers at time t to adjust the indoor temperature at the desired value (kW).

C. INTERNAL TEMPERATURE OF THE BUILDING

$$T_{in\ min}(t) \leq T_{in}(t) \leq T_{in\ max}(t) \quad \forall t \in \{0, 1, \dots, T\} \quad (19)$$

where $T_{in\ min}$, $T_{in\ max}$ are the minimum and maximum indoor temperatures (°C).

V. SIMULATION RESULTS

In this paper, a smart commercial building is given. The building is located in San Francisco city, US [6]. Two diesel generators K_1 (60 kW) and K_2 (80 kW), in addition to three

TABLE 6. ED case studies.

Case	ED	Fixed or variable curve of utility grid	Heating /Cooling load with air temperature impact
1	Day ahead ED	Fixed curve: case 1	-
2	Day-ahead ED	Fixed curve: case 2	-
3	Day-ahead ED	Variable curve	-
4	Five-minute-ahead ED	Fixed curve	-
5	Five-minute-ahead ED	Variable curve: case 1	-
6	Five-minute-ahead ED	Variable curve: case 2	-
7	Day-ahead ED	Fixed curve: case 1	Air temperature impact on heating load
8	Day-ahead ED	Variable curve	Air temperature impact on heating load
9	Day-ahead ED	Fixed curve: case 1	Air temperature impact on cooling load
10	Day-ahead ED	Variable curve	Air temperature impact on cooling load

PV power plants (35.1 kW for each) are given. Moreover, two Li-ion batteries are used. The proposed batteries are (100 kW × 0.5 h) × 2. Finally, the smart building can trade power (purchase or sell) based on the load demand and electricity prices. The parameters of diesel generators and the coefficients are given in table 4. The required thermal parameters are provided in table 5, where the efficiency of transferring the electrical power into thermal power is assumed as 50%.

To give a comprehensive investigation of the smart building system, ten case studies are given in table 6. The case studies discuss the ED operation under different dispatch intervals (five-minute ahead ED or day-ahead ED) and interconnect requirements, which mean fixed power curve or variable power curve of the utility grid. In addition, four cases investigate the improved model under air temperature impact. The proposed model is solved by GAMS.

A. DAY-AHEAD ED WITH FIXED POWER CURVE OF UTILITY GRID (CASE 1)

In this case, the total cost is USD 444.019. The load is delivered from the utility grid (load base), and the rest is supplied by the diesel generators and PV. Each diesel generator delivers a certain amount of power during the operation based on its generation cost. Therefore, the output power of the first generator is less than the output power of the second generator as presented in Fig. 4. The diesel generators produce more power, especially during the peak hours. In addition, power from discharging batteries. The outputs of DERs are displayed in Fig. 5 (a).

The batteries output is illustrated in Fig. 5 (b), the negative values mean the battery is discharging and vice versa. Charging hours occur during the off-peak time. However, the batteries charge three hours during the on-peak time (13:00 - 15:00 pm) due to the extra-generated power by DGs.

On the other hand, most of the discharging periods occur at the load peak time and during the on-peak time (high prices).

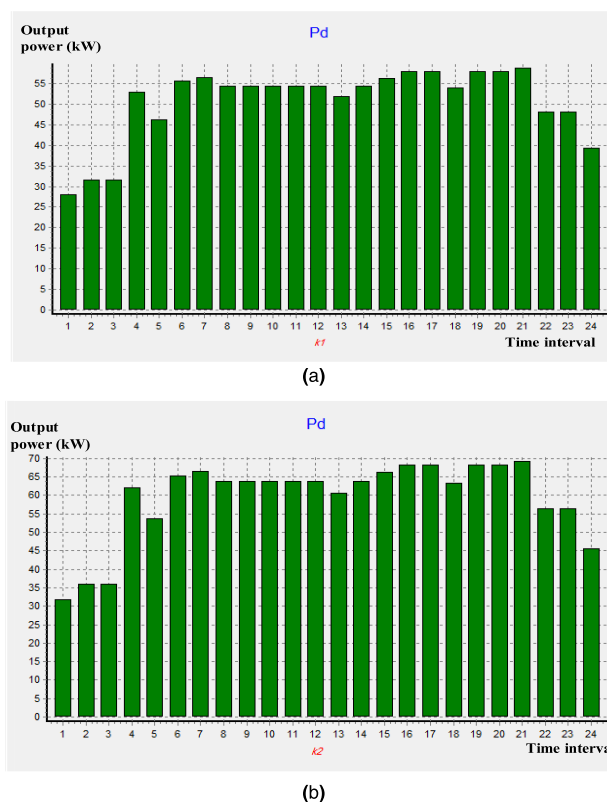
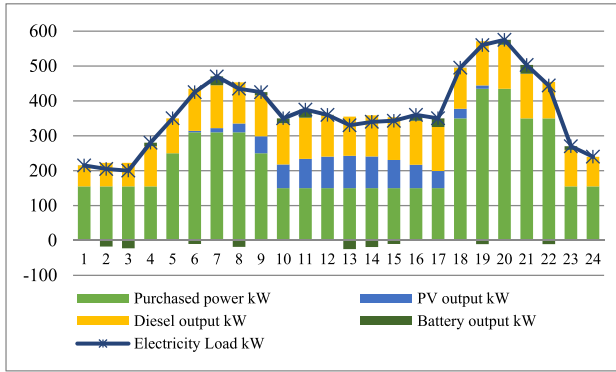


FIGURE 4. Output power of diesel generators (Pd). (a) K1. (b) K2.

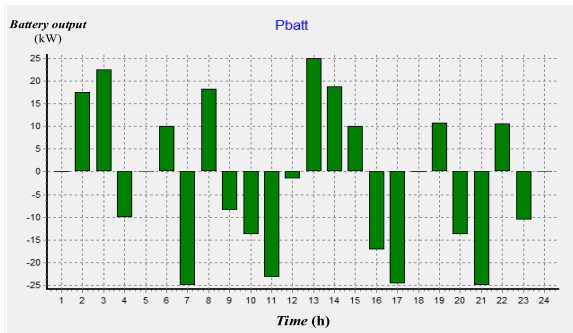
During the on-peak time, the PV and diesel outputs cannot meet the load demand. Therefore, the batteries discharge, such as 09:00-12:00 am. In this case, the microgrid will always purchase power from the utility grid.

B. FIVE-MINUTE-AHEAD ED WITH FIXED POWER CURVE OF UTILITY GRID (CASE 4)

In this case, each hour is divided into 12 periods in order to get the five-minute load curve. As a result, the cost is

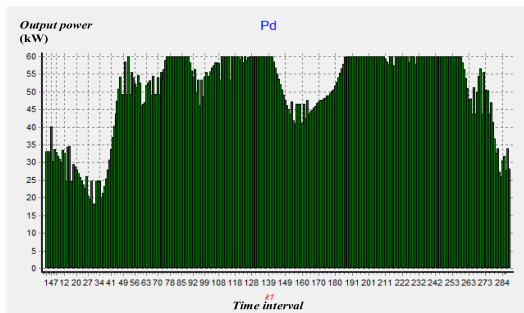


(a)

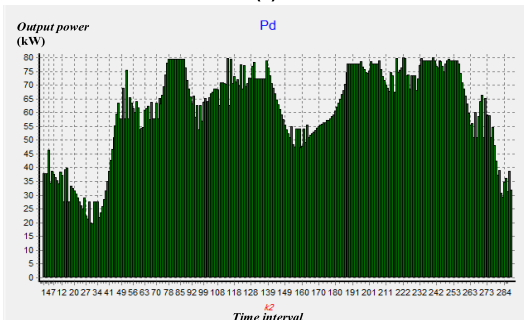


(b)

FIGURE 5. Day-ahead ED: (a) Output powers of DERs. (b) Battery output power.



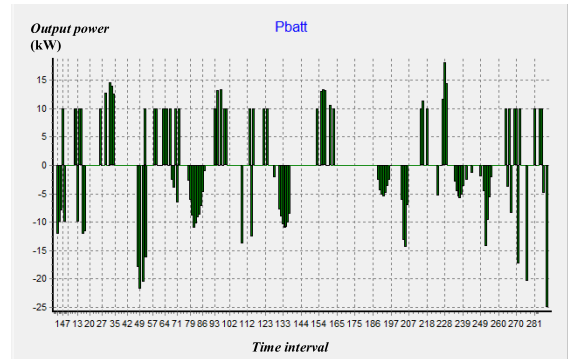
(a)



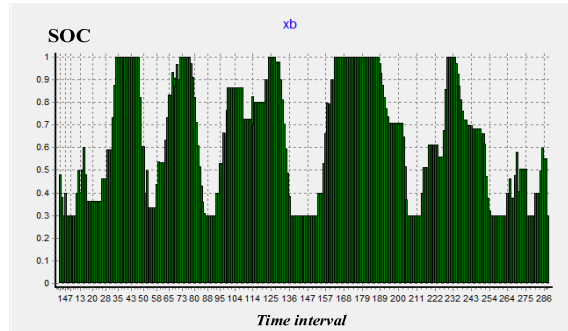
(b)

FIGURE 6. Output power of diesel generators (Pd). (a) K1. (b) K2.

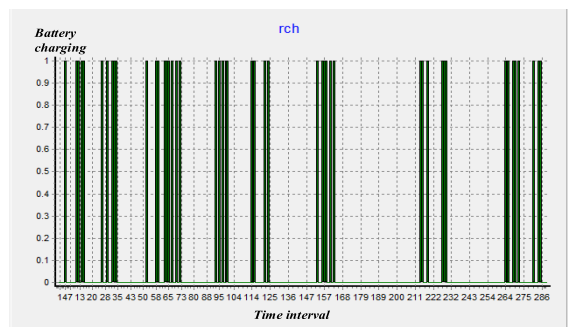
USD 441.969. The output power of the first generator is less than the output power of the second generator as presented in Fig. 6. The diesel generators should produce more power, especially during the demand peak periods. The charging



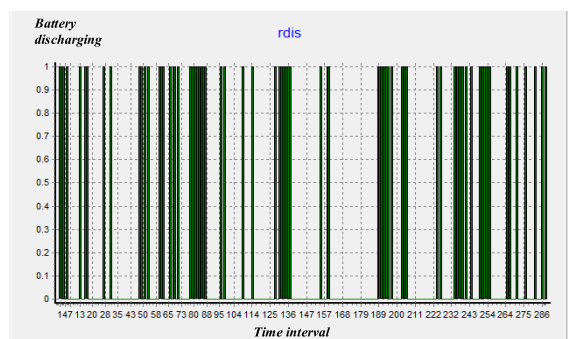
(a)



(b)



(c)



(d)

FIGURE 7. Battery out power and its control. (a) Battery output (Pbatt). (b) SOC. (c) Charging periods. (d) Discharging periods.

periods mostly happen during the off-peak time, which has low energy price. On the other hand, most of the discharging periods occur at the load peak time and during the on-peak time, which has high electricity price. The purchased power is not enough to meet the load. Therefore, if the power from PV and diesel generators in addition to the grid power cannot meet the load, the batteries will discharge.

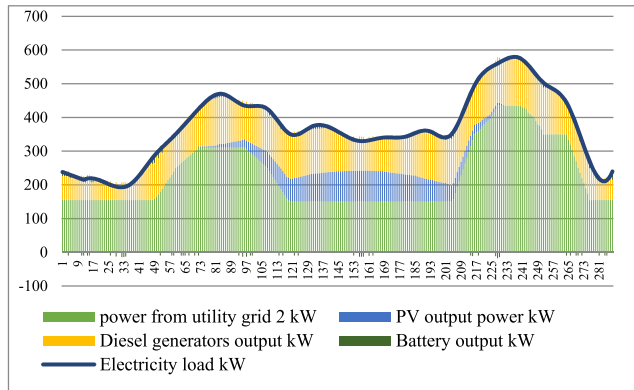


FIGURE 8. Five-minute-ahead ED: Output power of DERs.

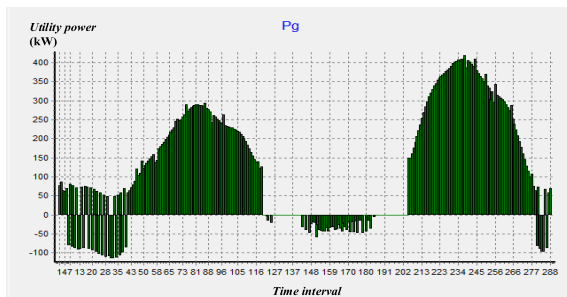


FIGURE 9. Purchased power (positive) and sold power (negative) from/to the grid (kW).

TABLE 7. Diesel generators parameters.

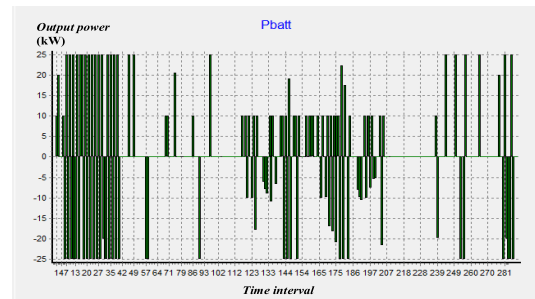
DG	a	b	c	P_{min}	P_{max}	M+O
	\$/kW ² h	\$/kWh	\$/h	kW	kW	\$/h
k1	0.00020	0.008	0.99	32	160	0.001265
k2	0.00016	0.009	1.1	36	180	0.001269

The batteries output is displayed in Fig. 7 (a). The control strategy, in addition to the charging and discharging periods are shown in Fig. 7 (b)-(d). Moreover, the outputs of DERs are illustrated in Fig. 8.

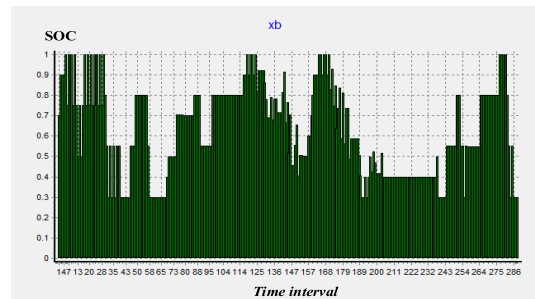
C. FIVE-MINUTE-AHEAD ED WITH VARIABLE CURVE OF UTILITY GRID (CASE 6)

In case 5 (Table 6), the power from the utility grid is variable. However, there is no sold power because the electricity price of power from grid is low comparing to power generated by diesel and other resources. The diesel generators produce power during the on-peak time (high power prices) and operate with their minimum power at the off-peak time (low energy price). Therefore, it is economic to purchase power from grid. With the given parameters, the diesel generators, in addition to PV and batteries are not enough to meet the load demand so the electricity must be purchased. Therefore, In this case, the parameters of the diesel generators are modified as shown in table 7. In this table, the power generation cost of diesel generators is less than the electricity price of the utility grid during the on-peak time.

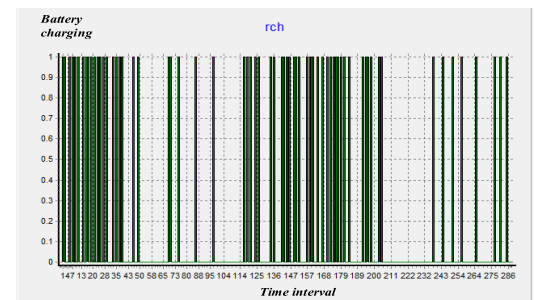
Fig. 9 displays the purchased and sold power. The positive values mean the power is purchased from grid and



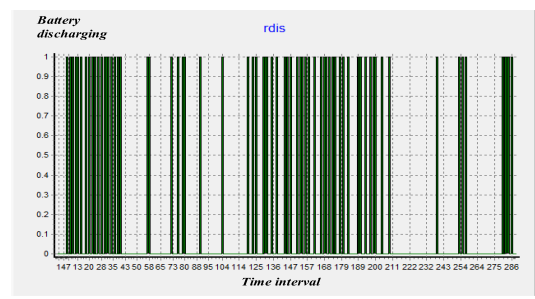
(a)



(b)



(c)



(d)

FIGURE 10. Battery out power and its control. (a) Battery output power (Pbatt). (b) SOC. (c) Charging periods. (d) Discharging periods.

negative values mean the power is sold. At the load peak time, the power is purchased from the grid in order to meet the high demand. However, at the on-peak time, the demand is not very high and the cost of power generation of diesel is less than the price of grid power. Therefore, the diesel generators produce more power, which in turn will be added to the PV output power. At the off-peak time, the power is sold, especially first hours of the day, where the load demand is low. On other hand, the extra-generated power can charge the batteries. Finally, the total cost dropped to USD 319.0005. The battery output and its control strategy, in addition to the

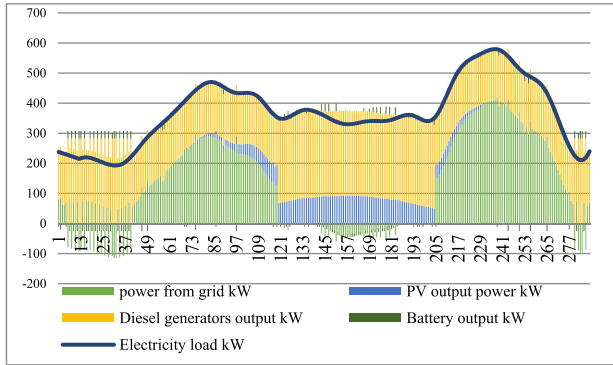


FIGURE 11. Five-minute-ahead ED: the output power of DERs.

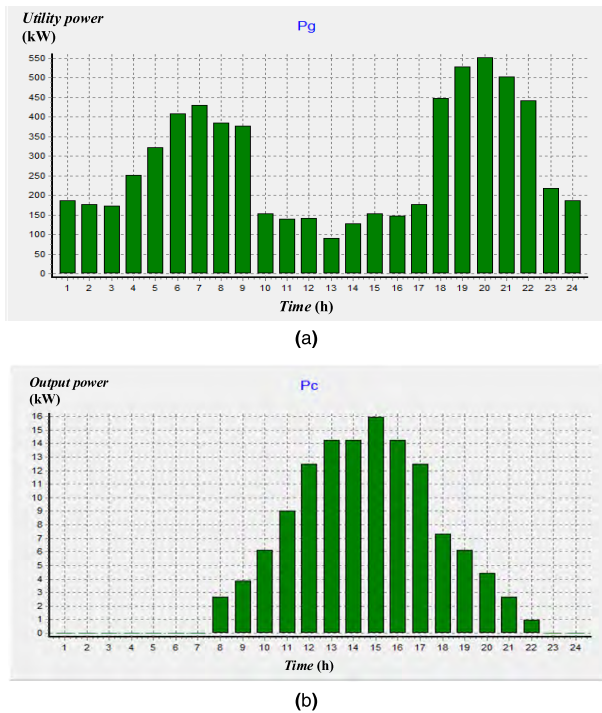


FIGURE 12. (a) Purchased power from grid (kW). (b) PC: Required power for cooling load (kW).

charging and discharging periods are shown in Fig. 10. The outputs of the DERs are illustrated in Fig. 11.

D. DAY-AHEAD ED CONSIDERING AIR TEMPERATURE IMPACT ON THE COOLING LOAD (CASE 10)

Similar to the case (6), the power from the utility grid is variable. However, considering the load demand and the produced power by DERs, the power from grid is always purchased as presented in Fig. 12 (a). In addition, the required power for the space cooling is obtained as given in Fig. 12 (b). The thermal load is related to the outdoor temperature and the internal required temperature.

The batteries output power and control strategy, in addition to the charging and discharging hours are displayed in Fig. 13. DERs outputs are illustrated in Fig. 14. When the thermal resistance of the building envelope: $R = 10$ ($^{\circ}\text{C}/\text{kW}$), the total cost will be USD 427.274.

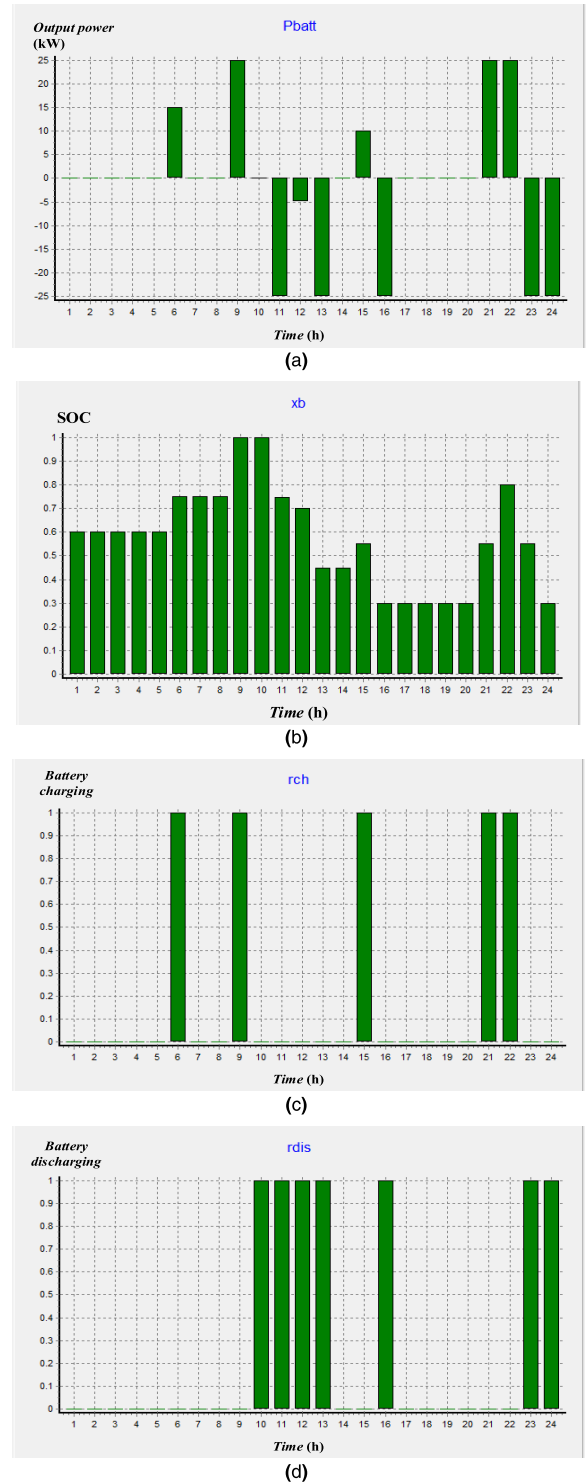


FIGURE 13. Battery out power and its control. (a) Battery output P_{bat} (kW). (b) SOC. (c) Charging hours. (d) Discharging hours.

E. RELATION BETWEEN THERMAL RESISTANCE AND TOTAL COST

The relation between R and the total cost is given in table 8. Although the higher values of R mean a lower cost, the thermal resistance value is restricted between minimum and maximum limits that cannot be exceeded. In winter,

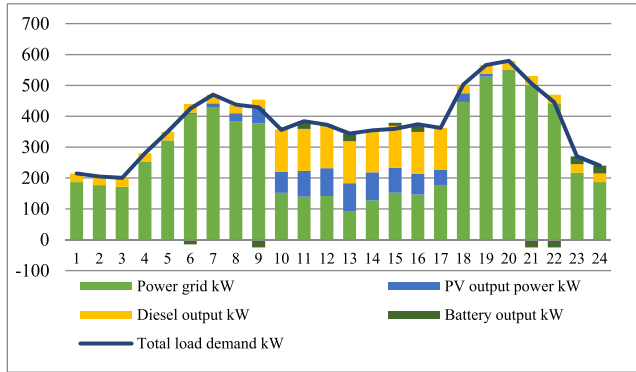


FIGURE 14. Day-ahead ED with air temperature impact: The output power of DERs.

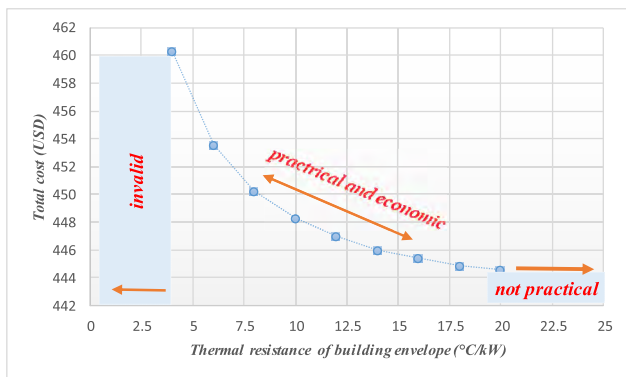


FIGURE 15. Relation between R and total cost.

TABLE 8. Relation between r and the total cost.

R (°C/kW)	Total cost (USD)
R ≥ 27	Not practical
20	444.532
18	444.863
16	445.374
14	445.998
12	446.952
10	448.233
8	450.226
6	453.519
4	460.258
2	Not valid

if the thermal resistance has a large value, which means the convective heat transfer from inside to outside the building through the walls and windows is low (even with very low outdoor temperatures), the required power for heating space will be low. On the contrary, if R has low value, the heating space will consume more power. In summer, if R has a large value, which means the convective heat transfer from the outside to inside across the building shell is low (even with high outdoor temperatures), the required power for cooling

TABLE 9. Summary of the case studies.

Case study	Total cost USD	charging	discharging
Case 1	444.019	9 hours	13 hours
Case 2	441.457	8 hours	12 hours
Case 3	418.245	5 hours	7 hours
Case 4	441.969	48 periods	80 periods
Case 5	413.483	17 periods	17 periods
Case 6	319.000	68 periods	71 periods
Case 7	448.233	10 hours	13 hours
Case 8	421.217	5 hours	7 hours
Case 9	453.612	8 hours	14 hours
Case 10	427.274	5 hours	7 hours

space will be low. If R is low, the cooling space will consume more power. The relation between R and total cost is clarified in Fig. 15.

A comparison between the ten case studies is displayed in table 9. The comparison takes into account the total cost, batteries charging time, and batteries discharging time. The table shows that EM operation with a variable power from utility grid is better and economic since it allows the microgrid to trade power.

VI. CONCLUSION AND FURTHER WORK

Microgrids for buildings combine the operation of power supply and load demand (electrical and thermal) to minimize the cost. In this paper, an improved EM operation was implemented for a microgrid, which includes several DERs on the supply side, in addition to HVAC and lighting loads on the demand side. A variable power curve of the utility grid allows the microgrid to trade power. Thus, ED operation will be economic. Secondly, the thermal loads for heating space and cooling space were achieved by adjusting the indoor temperature at a desired value. Finally, the smart building is insulated well. Therefore, the thermal resistance of the building envelope has a high value. The convective heat transfer across the building envelope will be low. The relation between the thermal resistance and the total cost is clarified. In further work, the model can be improved by including the unit commitment and considering other types of DERs, such as CHP and fuel cells. Furthermore, different types of energy storage devices can be investigated.

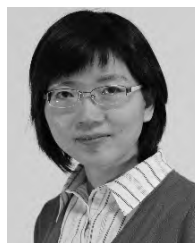
REFERENCES

- [1] H. M. Abou, X. Yang, and W. Chen, "Energy management of microgrid in smart building considering air temperature impact," in *Proc. IEEE Appl. Power Electron. Conf. Expo. (APEC)*, Mar. 2018, pp. 2398–2404.
- [2] A.-S. Malidin, C. Kayser-Bril, N. Maizi, E. Assoumou, V. Boutin, and V. Mazauric, "Assessing the impact of smart building techniques: A prospective study for France," in *Proc. Energy 2030 Conf.*, Nov. 2008, pp. 1–7.
- [3] Z. Xu, X. Guan, Q.-S. Jia, J. Wu, D. Wang, and S. Chen, "Performance analysis and comparison on energy storage devices for smart building energy management," *IEEE Trans. Smart Grid*, vol. 3, no. 4, pp. 2136–2147, Dec. 2012.

- [4] J. Wang, Z. Sun, Y. Zhou, and J. Dai, "Optimal dispatching model of smart home energy management system," in *Proc. Innov. Smart Grid Technol.-Asia (ISGT Asia)*, May 2012, pp. 1–5.
- [5] D. Bisen, H. M. Dubey, M. Pandit, and B. K. Panigrahi, "Solution of large scale economic load dispatch problem using quadratic programming and GAMS: A comparative analysis," *J. Inf. Comput. Sci.*, vol. 7, no. 3, pp. 200–211, 2012.
- [6] X. Guan, Z. Xu, and Q.-S. Jia, "Energy-efficient buildings facilitated by microgrid," *IEEE Trans. Smart Grid*, vol. 1, no. 3, pp. 243–252, Dec. 2010.
- [7] M. Tasdighi, H. Ghasemi, and A. Rahimi-Kian, "Residential microgrid scheduling based on smart meters data and temperature dependent thermal load modeling," *IEEE Trans. Smart Grid*, vol. 5, no. 1, pp. 349–357, Jan. 2014.
- [8] N. Augustine, S. Suresh, P. Moghe, and K. Sheikh, "Economic dispatch for a microgrid considering renewable energy cost functions," in *Proc. Innov. Smart Grid Technol. (ISGT)*, Jan. 2012, pp. 1–7.
- [9] C. Nayar, M. Tang, and W. Suponthana, "Wind/PV/diesel micro grid system implemented in remote islands in the Republic of Maldives," in *Proc. IEEE Int. Conf. Sustain. Energy Technol.*, Nov. 2008, pp. 1076–1080.
- [10] H. Morais, P. Kadar, P. Faria, Z. A. Vale, and H. M. Khodr, "Optimal scheduling of a renewable micro-grid in an isolated load area using mixed-integer linear programming," *Renew. Energy*, vol. 35, no. 1, pp. 151–156, 2010.
- [11] S. Chakraborty and M. G. Simoes, "PV-microgrid operational cost minimization by neural forecasting and heuristic optimization," in *Proc. IEEE Ind. Appl. Soc. Annu. Meeting*, Oct. 2008, pp. 1–8.
- [12] S. Jiang, W. Wang, H. Jin, and D. Xu, "Power management strategy for microgrid with energy storage system," in *Proc. 37th Annu. Conf. Ind. Electron. Soc. (IECON)*, Nov. 2011, pp. 1524–1529.
- [13] S. X. Chen, H. B. Gooi, and M. Q. Wang, "Sizing of energy storage for microgrids," *IEEE Trans. Smart Grid*, vol. 3, no. 1, pp. 142–151, Mar. 2012.
- [14] T. V. Chambers and J. Mutale, "Selection of diesel generators for small rural wind-diesel power systems," in *Proc. Universities Power Eng. Conf.*, vol. 1, Sep. 2006, pp. 51–55.
- [15] P. Mohanty, G. Bhuvaneshwari, and R. Balasubramanian, "Optimal planning and design of distributed generation based micro-grids," in *Proc. Ind. Inf. Syst. (ICIIS)*, Aug. 2012, pp. 1–6.
- [16] M. B. T. Molina, T. Gafurov, and M. Prodanović, "Proactive control for energy systems in Smart Buildings," in *Proc. Innov. Smart Grid Technol. (ISGT Eur.)*, Dec. 2011, pp. 1–8.
- [17] L. Martirano et al., "Demand side management in microgrids for load control in nearly zero energy buildings," *IEEE Trans. Ind. Appl.*, vol. 53, no. 3, pp. 1769–1779, Jun. 2017.
- [18] H. Kanchev, D. Lu, F. Colas, V. Lazarov, and B. Francois, "Energy management and operational planning of a microgrid with a PV-based active generator for smart grid applications," *IEEE Trans. Ind. Electron.*, vol. 58, no. 10, pp. 4583–4592, Oct. 2011.
- [19] M. Xie, W. Luo, P. Cheng, S. Ke, X. Ji, and M. Liu, "Multidisciplinary collaborative optimisation-based scenarios decoupling dynamic economic dispatch with wind power," *IET Renew. Power Gener.*, vol. 12, no. 6, pp. 727–734 2018.
- [20] Y. Zhang, N. Rahbari-Asr, J. Duan, and M. Y. Chow, "Day-ahead smart grid cooperative distributed energy scheduling with renewable and storage integration," *IEEE Trans. Sustain. Energy*, vol. 7, no. 4, pp. 1739–1748, Oct. 2016.
- [21] P. Stluka, D. Godbole, and T. Samad, "Energy management for buildings and microgrids," in *Proc. 50th IEEE Conf. Decis. Control Eur. Control Conf. (CDC-ECC)*, Dec. 2011, pp. 5150–5157.
- [22] P. H. Cheah, H. B. Gooi, and F. L. Soo, "Quarter-hour-ahead load forecasting for microgrid energy management system," in *Proc. IEEE Trondheim PowerTech*, Jun. 2011, pp. 1–6.
- [23] J. Tian, Z. Liu, J. Shu, J. Liu, and J. Tang, "Base on the ultra-short term power prediction and feed-forward control of energy management for microgrid system applied in industrial park," *IET Gener., Transmiss. Distrib.*, vol. 10, no. 9, pp. 2259–2266, 2016.
- [24] M. Yang, X. Chen, J. Du, and Y. Cui, "Ultra-short-term multistep wind power prediction based on improved EMD and reconstruction method using run-length analysis," *IEEE Access*, vol. 6, pp. 31908–31917, 2018.
- [25] W. Shi, X. Xie, C.-C. Chu, and R. Gadh, "Distributed optimal energy management in microgrids," *IEEE Trans. Smart Grid*, vol. 6, no. 3, pp. 1137–1146, May 2015.
- [26] M. Hijjo, F. Felgner, and G. Frey, "PV-battery-diesel microgrid design for buildings subject to severe power outages," in *Proc. IEEE PES Power Africa*, Jun. 2017, pp. 280–285.
- [27] C. Marnay, G. Venkataramanan, M. Stadler, A. S. Siddiqui, R. Firestone, and B. Chandran, "Optimal technology selection and operation of commercial-building microgrids," *IEEE Trans. Power Syst.*, vol. 23, no. 3, pp. 975–982, Aug. 2008.
- [28] M. Tasdighi, P. J. Salamati, A. Rahimikian, and H. Ghasemi, "Energy management in a smart residential building," in *Proc. IEEE 11th Int. Conf. Environ. Elect. Eng.*, May 2012, pp. 128–133.



MOHAMAD ABOU HOURAN received the B.S. degree in electrical engineering from Damascus University, Damascus, Syria, in 2010, and the M.S. degree from Xi'an Jiaotong University, Xi'an, China, in 2014, where he is currently pursuing the Ph.D. degree with the Department of Electrical Engineering. His research interests include microgrids, power market, electromagnet interference, and wireless power transfer.



WENJIE CHEN received the B.S., M.S., and Ph.D. degrees in electrical engineering from Xi'an Jiaotong University, Xi'an, China, in 1996, 2002, and 2006, respectively. From 2012 to 2013, she was with the Department of Electrical Engineering and Computer Science, University of Tennessee, Knoxville, TN, USA, as a Visiting Scholar. She then came back to Xi'an Jiaotong University, and engaged in the teaching and researches in power electronics. Since 2002, she has been a Member of the Faculty of School of Electrical Engineering, Xi'an Jiaotong University, where she is currently a Professor. Her current research interests include electromagnetic interference, active filters, and power electronic integration.



MINGHUI ZHU received the B.Eng. and M.Sc. degrees in electrical engineering from Xi'an Jiaotong University, Xi'an, China, in 2013 and 2016, respectively. He is currently with the State Grid Shaanxi Electric Power Research Institute, Xi'an, as a Researcher. His research interests include control and the optimization of power system and electric market.



LIYU DAI received the B.S. degree in electrical engineering from Fuzhou University, Fuzhou, China, in 2017. He is currently pursuing the M.S. degree in power electronics with the School of Electrical Engineering, Xi'an Jiaotong University. His research interests include electromagnetic interference and active filters.

...